

High-purity transmission of a slow light odd mode in a photonic crystal waveguide

Jun Tan,¹ Ming Lu,² Aaron Stein,² and Wei Jiang^{1,3,*}

¹Department of Electrical and Computer Engineering, Rutgers University, Piscataway, New Jersey 08854, USA

²Center for Functional Nanomaterials, Brookhaven National Laboratory, Upton, New York 11973, USA

³Institute for Advanced Materials, Devices, and Nanotechnology, Rutgers University, Piscataway, New Jersey 08854, USA

*Corresponding author: wjiangnj@rci.rutgers.edu

Received May 4, 2012; revised June 5, 2012; accepted June 8, 2012;
posted June 11, 2012 (Doc. ID 166625); published July 25, 2012

We demonstrate a novel scheme to control the excitation symmetry for an odd mode in a photonic crystal waveguide and investigate the spectral signature of this slow light mode. An odd-mode Mach-Zehnder coupler is introduced to transform mode symmetry and excite a high-purity odd mode with 20 dB signal contrast over the background. Assisted by a mixed-mode Mach-Zehnder coupler, slow light mode beating can be observed and is utilized to determine the group index of this odd mode. With slow light enhancement, this odd mode can help enable novel miniaturized devices such as one-way waveguides. © 2012 Optical Society of America

OCIS codes: 130.5296, 230.5298.

Photonic crystal waveguides (PCWs) [1–5] can modify light propagation and dispersion characteristics through their periodic structures and thus have important applications in communications and sensing. Particularly, the slow light effect in a PCW can significantly enhance light-matter interaction [6–8], as demonstrated in significant reduction of interaction lengths for PCW-based modulators and switches [9–11]. To date, most of the PCW research has been focused on the TE-like mode with even symmetry. However, a PCW often has an odd TE-like mode inside the photonic bandgap exhibiting the slow light effect as well. This odd mode can potentially open up the opportunities for mode-symmetry-based novel devices, such as one-way waveguides that exploit indirect interband photonic transitions between even and odd modes [12]. The slow light effect in PCWs can help reduce the interaction length for such transitions, enabling ultracompact devices. To utilize this odd mode in any device, it is crucial to control its excitation symmetry and understand its slow light spectral characteristics. Normally, this odd mode does not exhibit itself evidently in the PCW transmission spectrum because its odd symmetry prohibits its excitation by the fundamental even mode of a conventional waveguide typically used at input. Symmetry-breaking coupling structure imperfections sometimes may induce some coupling to this odd mode, causing a decrease of PCW transmission in the odd mode band [13,14]. Here we demonstrate a novel scheme to control the excitation symmetry for high-purity transmission of this odd mode and investigate the spectral signatures under various excitation symmetries.

Consider a W1 PCW formed on a silicon-on-insulator (SOI) wafer by removing a row of air holes in a hexagonal lattice with lattice constant $a = 400$ nm, hole radius $r = 0.325a$, and Si slab thickness $t = 260$ nm. The band diagram in Fig. 1(a) is calculated by three-dimensional (3D) plane wave expansion [15] (with $>1 \mu\text{m}$ top/bottom claddings and six rows of holes per side). Below the lightline (for the oxide bottom cladding), the even TE-like mode has a flat dispersion relation with group index $n_g > 50$ and a narrow bandwidth (<4 nm). In contrast, below the lightline, the odd TE-like mode has a much wider bandwidth, ~ 20 nm, with n_g down to ~ 15 . Such a mod-

erate n_g range is favorable for many applications as various types of losses are reduced at lower n_g [5,15–17]. Furthermore, the dispersion relation of the TM-like guided mode usually crosses that of the even mode [5], as seen in Fig. 1(a). But the TM-like mode does not cross the odd mode in the region below the lightline in Fig. 1(a). For $\omega a/2\pi c = 0.28$ – 0.286 , only the odd mode is below the lightline.

Systematic simulations show that as the hole radius increases, the odd-mode band edge moves up faster than the TM cutoff, as shown in Fig. 1(b). For a sufficiently large r , the TM cutoff is below the odd-mode band edge; thus the two modes do not cross each other below the lightline, helping avoid their intercoupling due to asymmetric top and bottom claddings. However, as r increases, the transmission bandwidth bounded by the band edge and the cutoff decreases for both the even and odd modes, as shown in Fig. 1(b). Hence, this work focuses on the intermediate r case shown in Fig. 1(a), which shows a sufficient clearance between the odd-mode band edge and the TM cutoff, and a sufficiently wide bandwidth.

Excitation of this odd PCW mode is usually deterred by the opposite symmetry of the fundamental even mode of a Si waveguide. To solve this problem, we employ a

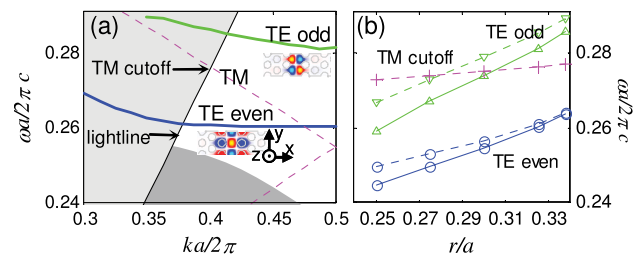


Fig. 1. (Color online) PCW photonic band structures. (a) Band diagram for $r = 0.325a$. The dark grey region indicates the lower photonic band. H_z field profiles for even and odd modes at $k = \pi/a$ are shown in the insets (PCW axis along y); (b) variation of the band edge and cutoff of even (blue) and odd (green) TE-like modes with hole radius. For each TE-like mode, the lower line (solid) gives the band edge; the upper line (dashed) gives the cutoff frequency where a mode crosses the lightline. The TM cutoff is also shown.

Report Documentation Page				Form Approved OMB No. 0704-0188	
Public reporting burden for the collection of information is estimated to average 1 hour per response, including the time for reviewing instructions, searching existing data sources, gathering and maintaining the data needed, and completing and reviewing the collection of information. Send comments regarding this burden estimate or any other aspect of this collection of information, including suggestions for reducing this burden, to Washington Headquarters Services, Directorate for Information Operations and Reports, 1215 Jefferson Davis Highway, Suite 1204, Arlington VA 22202-4302. Respondents should be aware that notwithstanding any other provision of law, no person shall be subject to a penalty for failing to comply with a collection of information if it does not display a currently valid OMB control number.					
1. REPORT DATE 25 JUL 2012		2. REPORT TYPE		3. DATES COVERED 00-00-2012 to 00-00-2012	
4. TITLE AND SUBTITLE High-purity transmission of a slow light odd mode in a photonic crystal waveguide				5a. CONTRACT NUMBER	
				5b. GRANT NUMBER	
				5c. PROGRAM ELEMENT NUMBER	
6. AUTHOR(S)				5d. PROJECT NUMBER	
				5e. TASK NUMBER	
				5f. WORK UNIT NUMBER	
7. PERFORMING ORGANIZATION NAME(S) AND ADDRESS(ES) Rutgers University, Department of Electrical and Computer Engineering, Piscataway, NJ, 08854				8. PERFORMING ORGANIZATION REPORT NUMBER	
9. SPONSORING/MONITORING AGENCY NAME(S) AND ADDRESS(ES)				10. SPONSOR/MONITOR'S ACRONYM(S)	
				11. SPONSOR/MONITOR'S REPORT NUMBER(S)	
12. DISTRIBUTION/AVAILABILITY STATEMENT Approved for public release; distribution unlimited					
13. SUPPLEMENTARY NOTES					
14. ABSTRACT					
15. SUBJECT TERMS					
16. SECURITY CLASSIFICATION OF:			17. LIMITATION OF ABSTRACT Same as Report (SAR)	18. NUMBER OF PAGES 3	19a. NAME OF RESPONSIBLE PERSON
a. REPORT unclassified	b. ABSTRACT unclassified	c. THIS PAGE unclassified			

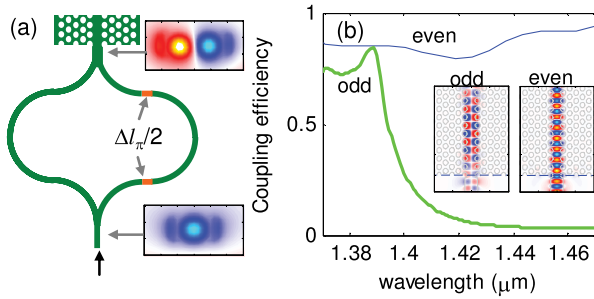


Fig. 2. (Color online) FDTD simulation results; (a) schematic of the MZC structure. The right arm has two extra waveguide segments (in orange) with a combined length of $(\Delta l)_\pi$. The input and output E_x field profiles (cross section) are shown in the insets (200 nm per division on axes); (b) PCW coupling efficiency. Insets: coupled E_x field patterns at 1390 nm. Light (in odd or even mode) enters from a Si waveguide at the bottom of each figure and into a PCW upward.

two-step approach. First, a Mach-Zehnder coupler (MZC) whose two arms have a phase difference of π is utilized to transform mode symmetry and excite an odd mode in a wide (multimode) Si wire waveguide; then this odd mode is coupled to the odd mode of the PCW. To create π phase difference in this *odd-mode* MZC, its two arms can be designed to have a length difference of $(\Delta l)_\pi = \lambda/2n_{\text{eff}}$, where n_{eff} is the effective index of the Si waveguide. Finite difference time-domain (FDTD) simulation has been performed to confirm that such a MZC produces an odd mode in a wide output waveguide, as shown in Fig. 2(a). The input and output waveguide widths are 400 and 700 nm, respectively. The coupling between the odd mode of a Si wire waveguide (700 nm wide) and that of the PCW is also simulated. Simulation results in Fig. 2(b) show coupling efficiencies up to $\sim 84\%$ (~ 0.75 dB) for the odd mode. The field pattern in Fig. 2(b), left inset, confirms that the coupled PCW mode is an odd mode. The fundamental even mode of a Si wire waveguide couples into the PCW with inconsequential change of coupling efficiency for the spectral range in Fig. 2(b). The field pattern in Fig. 2(b), right inset, indicates that the coupled mode has even symmetry. Indeed, this mode is an even TE-like mode above the lightline. The E_x field has been shown in Fig. 2 for direct comparison with the modes of the conventional Si waveguide, whose TE modes are commonly visualized by E_x (note E_x and H_z have the same symmetry with respect to x).

The PCW structure is fabricated on a SOI wafer with a 2 μm buried oxide layer and a 260 nm top Si layer according to the parameters used in Fig. 1(a). The structure is patterned by a JEOL JBX-6300FS high-resolution e-beam lithography system, operating at 100 keV, on a 100 nm thick layer of ZEP 520A e-beam resist. Then the pattern is transferred to the Si layer by an Oxford Plasmalab 100 ICP etcher. Figure 3 is a scanning electron microscope (SEM) image of the fabricated structure. Two MZCs with a 10 μm bending radius are connected through 700 nm wide Si waveguides of 1 μm length to both ends of the PCW.

To measure transmission spectra, light from a superluminescent LED with a spectral range of about 80 nm is coupled to the TE mode of Si access waveguides (tapered to 4 μm at chip edges) via lensed fibers. A polarizer is used at the output end to block TM polarization.

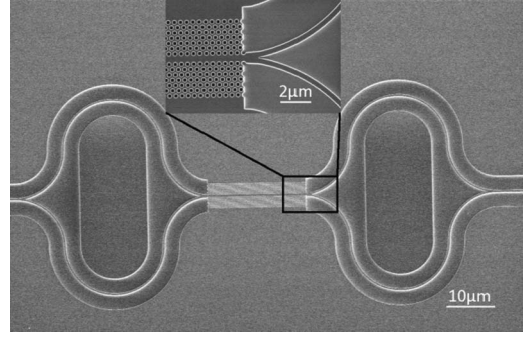


Fig. 3. SEM image of a PCW with odd-mode MZCs. Inset: close-up view of the coupling region at one end of the PCW.

The PCW insertion loss is measured with reference to a Si wire waveguide. Figure 4(a) shows the spectrum of a PCW with odd-mode MZCs. A substantial transmission bandwidth is observed, approximately 22 nm at 10 dB below the peak. The contrast between the transmitted mode and background is >20 dB. The peak insertion loss is about -4 dB. Separate measurements show that each MZC contributes ~ 1 dB. Thus the loss due to the PCW is estimated at ~ 2 dB. For comparison, the spectrum of a directly coupled PCW without MZCs is shown in Fig. 4(b). The transmission is due to the leaky even TE-like mode as simulated in Fig. 2(b). Figure 4(b) also shows the PCW transmission with MZCs whose two arms have a length difference Δl deliberately designed to be 50% greater than $(\Delta l)_\pi$. Such a *mixed-mode* MZC offers a symmetry configuration that can excite a mixture of even and odd modes according to $I_\pm \propto (1/2)[1 \pm \cos(2\pi n_{\text{eff}} \Delta l / \lambda)]$. As such, the background transmission due to the even mode rises. In the odd-mode band, the mixed-mode spectrum oscillates strongly due to the beating of two modes. Figures 4(a) and 4(b) illustrate that distinctive spectral signatures can be observed with controlled excitation symmetries.

The mode-beating pattern of the mixed-mode spectrum contains important information of the odd mode. The beating period is related to the group indices of even and odd modes through $\Delta\lambda = \lambda^2 / (n_{g,\text{odd}} - n_{g,\text{even}})L$, where L is the PCW length. Simulation indicates that $n_{g,\text{even}}$ is virtually a constant (~ 5) in the odd-mode band. Thus the chirped beating periods are due to the dispersion of $n_{g,\text{odd}}$. We have calculated $\Delta n_g = n_{g,\text{odd}} - n_{g,\text{even}}$ from the mixed-mode spectrum and plotted it in Fig. 4(c). The peak spacing and valley spacing of the spectrum give two sets of Δn_g data, plotted by circles and crosses

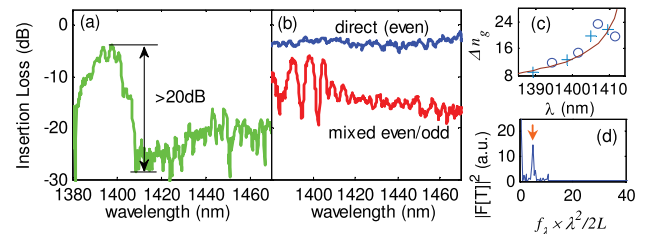


Fig. 4. (Color online) Transmission spectra for 20 μm long PCWs: (a) with odd-mode MZCs; (b) direct transmission without MZC and transmission with mixed-mode MZCs; (c) Δn_g obtained from the mixed-mode spectrum; the solid line delineates the trend; (d) Fourier transform of the transmission spectrum of another directly coupled PCW (the peak position gives $n_{g,\text{even}}$).

respectively. They agree with each other, as expected. Note that the Δn_g value obtained from two adjacent peaks (valleys) is assigned to the midpoint wavelength in between. Further, $n_{g,\text{even}} = 4.9$ is obtained in Fig. 4(d) through the Fourier transform [18] of the transmission spectrum of another directly coupled PCW with more obvious spectral ripples. Note that the Fourier frequency f_λ is just the inverse of the spectral oscillation period $\delta\lambda$, thus $n_{g,\text{even}} = f_\lambda \times \lambda^2 / 2L$. Based on Figs. 4(c) and 4(d), we find $n_{g,\text{odd}} = \Delta n_g + n_{g,\text{even}}$ in the range of 14 to 29. Note that the Fabry–Perot (F-P) oscillation amplitude in Fig. 4(a) is relatively weak. In contrast, the mode-beating amplitude of the mixed-mode spectrum in Fig. 4(b) is much higher and more robust against noise, which facilitates the evaluation of $n_{g,\text{odd}}$. Also note that in Fig. 4(a), the background transmission increases discernibly beyond 1430 nm due to the dispersive effect in the odd-mode MZC, which modifies the phase shift difference between the two arms as λ deviates far from the designed value (1390 nm). The TM-like mode (guided for $\lambda > 1.45 \mu\text{m}$) may also contribute to the background at long wavelengths. However, these effects are much weaker for 1380–1415 nm.

Although this work focuses on PCWs on a SOI chip, the MZC and the mode-beating-based $n_{g,\text{odd}}$ measurement method can be adapted to the cases of air-bridge or oxide-covered PCWs and coupled-cavity PCWs, where interesting anomalous propagation related to an odd mode has been observed [19]. It would be interesting also to explore a refined design to optimize the bandwidth and the slow-down of light together for this odd mode. Detailed discussion of these possibilities is beyond the scope of this work. The odd-mode wavelength can also be shifted to ~ 1550 nm or other values (depending on specific applications) by changing the lattice constant. In a SOI PCW, there is some coupling between the TE-like guided modes and the TM-like photonic crystal bulk modes due to asymmetric top/bottom claddings. Prior work on the even mode has demonstrated that reducing n_g can reduce the loss due to such coupling [5]. This odd mode has a much lower n_g , ~ 14 , than the normal even mode ($n_g \sim 50$) below the lightline. This helps to reduce the coupling to the TM-like bulk modes. For many PCW devices operating at a short length $< 80 \mu\text{m}$ [9,10], the propagation loss of the odd mode is expected to be reasonable. Lastly, the understanding of the slow light and mode-beating characteristics of this odd mode, as well as the controlled excitation and $n_{g,\text{odd}}$ characterization schemes developed here, can facilitate the development of mode-symmetry-based novel devices, such as one-way waveguides that involve active transition and passive conversion between even and odd modes [12]. Slow light can help reduce device interaction length. Note that previously demonstrated conventional waveguide mode converters employed branching waveguides [20,21] or multimode interference couplers [22]. Photonic-crystal-based mode converters have also been designed [23]. Here, the odd-mode MZC is focused on transforming mode symmetry to attain a high-purity odd mode, and the mixed-mode MZC offers a symmetry configuration for coherent mixing of even and odd modes, which enables $n_{g,\text{odd}}$ measurement through slow-light mode beating.

As a side note, beating between two degenerate modes in a periodically patterned microring resonator has recently been observed, but the resonant wavelength spacing is not affected by beating [24].

In summary, we have experimentally demonstrated the control of excitation symmetry for an odd TE-like mode in a PCW. An odd-mode MZC is utilized to selectively excite the odd mode with a contrast > 20 dB over the background. Assisted by a mixed-mode MZC, slow light mode beating is observed and is utilized to measure the group index of this odd mode.

This work is supported in part by AFOSR Grant No. FA9550-10-C-0049. This research is carried out in part at the Center for Functional Nanomaterials, Brookhaven National Laboratory, which is supported by the U.S. Department of Energy, Office of Basic Energy Sciences, under Contract No. DE-AC02-98CH10886.

References

1. M. Loncar, D. Nedeljkovic, T. Doll, J. Vuckovic, A. Scherer, and T. P. Pearsall, *Appl. Phys. Lett.* **77**, 1937 (2000).
2. S. Y. Lin, E. Chow, S. G. Johnson, and J. D. Joannopoulos, *Opt. Lett.* **25**, 1297 (2000).
3. M. Notomi, A. Shinya, K. Yamada, J. Takahashi, C. Takahashi, and I. Yokohama, *IEEE J. Quantum Electron.* **38**, 736 (2002).
4. W. T. Lau and S. H. Fan, *Appl. Phys. Lett.* **81**, 3915 (2002).
5. A. H. Atabaki, E. S. Hosseini, B. Momeni, and A. Adibi, *Opt. Lett.* **33**, 2608 (2008).
6. M. Soljacic and J. D. Joannopoulos, *Nat. Mater.* **3**, 211 (2004).
7. T. F. Krauss, *J. Phys. D* **40**, 2666 (2007).
8. T. Baba, *Nat. Photon.* **2**, 465 (2008).
9. Y. A. Vlasov, M. O'Boyle, H. F. Hamann, and S. J. McNab, *Nature* **438**, 65 (2005).
10. L. L. Gu, W. Jiang, X. N. Chen, L. Wang, and R. T. Chen, *Appl. Phys. Lett.* **90**, 071105 (2007).
11. D. M. Beggs, T. P. White, L. O'Faolain, and T. F. Krauss, *Opt. Lett.* **33**, 147 (2008).
12. Z. Yu and S. H. Fan, *Nat. Photon.* **3**, 91 (2009).
13. B. Cluzel, D. Gerard, E. Picard, T. Charvolin, V. Calvo, E. Hadji, and F. de Fornel, *Appl. Phys. Lett.* **85**, 2682 (2004).
14. E. Dulkeith, S. J. McNab, and Y. A. Vlasov, *Phys. Rev. B* **72**, 115102 (2005).
15. W. Song, R. A. Integlia, and W. Jiang, *Phys. Rev. B* **82**, 235306 (2010).
16. E. Kuramochi, M. Notomi, S. Hughes, A. Shinya, T. Watanabe, and L. Ramunno, *Phys. Rev. B* **72**, 161318 (2005).
17. L. O'Faolain, S. A. Schulz, D. M. Beggs, T. P. White, M. Spasenovic, L. Kuipers, F. Morichetti, A. Melloni, S. Mazoyer, J. P. Hugonin, P. Lalanne, and T. F. Krauss, *Opt. Express* **18**, 27627 (2010).
18. M. H. Shih, W. J. Kim, W. Kuang, J. R. Cao, H. Yukawa, S. J. Choi, J. D. O'Brien, P. D. Dapkus, and W. K. Marshall, *Appl. Phys. Lett.* **84**, 460 (2004).
19. H. H. Tao, C. Ren, Y. Z. Liu, Q. K. Wang, D. Z. Zhang, and Z. Y. Li, *Opt. Express* **18**, 23994 (2010).
20. B. T. Lee and S. Y. Shin, *Opt. Lett.* **28**, 1660 (2003).
21. M. W. Pruessner, J. B. Khurgin, T. H. Stievater, W. S. Rabinovich, R. Bass, J. B. Boos, and V. J. Urick, *Opt. Lett.* **36**, 2230 (2011).
22. J. Leuthold, P. A. Besse, E. Gamper, M. Dulk, S. Fischer, and H. Melchior, *Electron. Lett.* **34**, 1598 (1998).
23. Y. Jiao, S. H. Fan, and D. A. B. Miller, *Opt. Lett.* **30**, 141 (2005).
24. J. Y. Lee and P. M. Fauchet, *Opt. Lett.* **37**, 58 (2012).